HAL
open science

Tube Drawing Process Modelling By A Finite Element Analysis

Muriel Palengat, Grégory Chagnon, Christophe Millet, Denis Favier

To cite this version:

Muriel Palengat, Grégory Chagnon, Christophe Millet, Denis Favier. Tube Drawing Process Modelling By A Finite Element Analysis. 9th international conference on numerical methods in industrial forming processes, Jun 2007, Porto, Portugal. hal-01978983

HAL Id: hal-01978983

https://hal.science/hal-01978983v1

Submitted on 30 Jan 2019

HAL is a multi-disciplinary open access archive for the deposit and dissemination of scientific research documents, whether they are published or not. The documents may come from teaching and research institutions in France or abroad, or from public or private research centers.

L'archive ouverte pluridisciplinaire **HAL**, est destinée au dépôt et à la diffusion de documents scientifiques de niveau recherche, publiés ou non, émanant des établissements d'enseignement et de recherche français ou étrangers, des laboratoires publics ou privés.

Tube Drawing Process Modelling By A Finite Element Analysis

M. Palengat [1,2], G. Chagnon [1,*], C. Millet [2], D. Favier [1]

1 Laboratoire Sols, Solides, Structures, UMR CNRS 5521, Universités de Grenoble, BP 53, 38041 Grenoble Cedex 09, France
2 Minitubes SA, 21 rue Vaujany, 38100 Grenoble, France
**Corresponding author: gregory.chagnon@hmg.inpg.fr*

Abstract. Drawing process is used in manufacturing thin-walled tubes, while reducing progressively their wall thickness and their inner and outer diameters. In this paper a stainless steel 316LVM and a cobalt alloy L605 are studied with two drawing processes, hollow sinking and plug drawing. This study gets into different issues including elastoplastic behaviour, contacts, friction and numerical convergence. Experimental drawings are realized on a testing bench where forces and dimensional data are recorded. In a first approach, tensile tests lead up to apply an elastoplastic constitutive equation with an isotropic hardening law. In simulations, an axisymetric steady-state model, with numeric stabilization if needed, is used. Numerical results are compared with experimental results. Finally, in spite of some defaults, this study shows that finite element modelling is able to foresee accurately the behaviour of a tube during a drawing process. A better understanding and modelling of the mechanical behaviour of materials will improve the FEM simulation results.

Keywords: Tube drawing, finite element analysis, elastoplasticity, experimental results.
PACS:

INTRODUCTION

Thin-walled tubes are manufactured with the tube drawing process, reducing progressively inner and outer diameters together with wall thickness. In most cases, industries develop empirically their production. As it induces many experiments, this method costs a lot of time and energy. Numerical simulation is an alternative solution that we explore in this paper. A first step is to characterize the material with simple mechanical tests available for tube geometries; then numerical simulation will allow to test the feasibility of drawing passes and to give an optimized range of production. This will reduce the number of experimental tests and then the cost of development.

Few works exist on tube drawing process but different studies have already been realized to optimize tools' geometries [1] and observe stresses and strains with several drawing processes [2, 3, 4]. Karnezis and Farrugia [5] developed an optimization procedure based on the Cockcroft-Latham workability failure criterion.

The aim of the present study is to model tube drawing with a finite element (FE) analysis. Two drawing processes, hollow sinking and fixed plug drawing are studied with a stainless steel (316L) and a cobalt-based alloy (L605).

Accurate modeling results imply to have a deep knowledge of parameters that affect the process as tools and tubes geometries and of materials behaviour. The main difficulties are due to large deformations and complex contact conditions which must be well characterized and which involve numerical convergence problems. In a first part, drawing experiments performed on drawbenches are described, the second part detail the modelling hypotheses including constitutive equations to describe the materials mechanical behaviour. In a third part, experimental measurements and results predicted by the FE model are compared and discussed.

DRAWING EXPERIMENTS

Tube drawings were realized on a testing bench (Figure 1) with two materials: a stainless steel (316LVM) and a cobalt-based alloy (L605). First hollow sinking will be introduced and second the drawing process with fixed plug. The simulation of

these processes will be realized further and compared with these experimental data.

FIGURE 1. Drawbench.

Hollow Sinking

A first series of measurements has been done on hollow sinking tests. The process is presented in Figure 2. A tube is introduced in a die which has a diameter smaller than the tube outer diameter. Two diamond conical dies with a half angle of 25° or 14° respectively have been used. The drawing speed is 2m/min. A load cell takes place on the drawing device to record the drawing force.

For the 316LVM alloy, three tests have been realized with different die diameters. The initial tube inner and outer diameters were 2.00 mm and 2.37 mm, respectively. For the L605 alloy, these diameters were 1.81 mm and 2.06 mm, respectively. Details of experiments data (initial tube and die geometries) are listed in table 1.

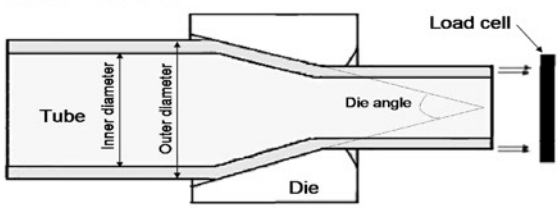

FIGURE 2. Hollow sinking

The shape of the time-drawing force curve is composed of three parts. When the tube enters in the die, the drawing force increases quickly and reaches a steady state where the force is practically constant. Finally, the drawing force decreases when the tube exits the die. In the following, we will consider only the steady state. Besides the tube extremities are not used for industrial applications as they do not have the same material and geometrical properties. In fact, they are only used to fix the tube.

Drawing forces during the steady state and final dimensions were recorded and are summarized in table 1. Each test has been performed twice and results have been identical, accurate to within 0.01mm.

TABLE 1. Experimental measurements for hollow sinking.

Initial Tube (Φext×Φint) mm	Die Angle	Die Diameter mm	Final Tube (Φext×Φint) mm	Drawing Force daN
		316LVM		
2.37×2.00	25°	1,50	1.47×1.07	50
2.37×2.00	25°	1.73	1.70×1.30	40
2.37×2.00	25°	2.04	1.98×1.60	25
		L605		
2.06×1.81	25°	1.45	1.46×1.18	37
2.06×1.81	25°	1.50	1.49×1.21	32
2.06×1.81	25°	1.60	1.59×1.31	26
2.06×1.81	14°	1.58	1.59×1.32	29

Drawing With Fixed Plug

Drawings with fixed plug, illustrated in Figure 3, have been performed. The process is similar to hollow sinking except that a fixed plug is inserted inside the tube to impose the final inner diameter. The plug is hold by a metal rod on which a load cell records the force applied on the plug. A diamond conical die with a half angle of 25° and a tungsten carbide plug with a half angle of 1° have been used.

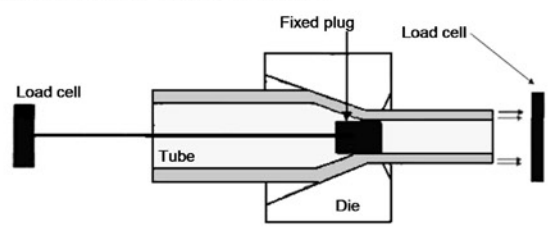

FIGURE 3. Drawing with fixed plug.

One fixed plug drawing experiment has been performed for each of the two materials. In both cases, the same initial tubes as for hollow sinking have been used. For each test, initial and final dimensions, tools geometries, drawing forces and also forces applied on plug have been recorded and summed up in the table 2.

TABLE 2. Experimental measurements for drawing with fixed plug.

Material	Initial Tube (Φext×Φint) mm	Die Diameter mm	Plug Diameter Mm	Final Tube (Φext×Φint) mm	Drawing Force daN	Plug Force daN
316LVM	2.37×2.00	1,80	1.50	1.79×1.51	62	12
L605	2.06×1.81	1.60	1.50	1.60×1.49	47	12

NUMERICAL SIMULATION

Hypothesis

As geometries and loading conditions are axially symmetric, an axisymmetric model is used. The steady-state condition is the dominating phase in tube drawing. Then, only the steady state and a part of the total tube's length are considered in a first approach.
Tube drawing provides large deformation and then plasticity. Inelastic phenomena and friction generate heat but in a first approach it is assumed that the materials' behaviours are temperature independent. Thus the model does not take into account temperature.
Besides, during drawing, strain rates are of the order of 10 to 100 s^{-1}. However, the tests are at room temperature T (300K), and the melting point Tf of the studied alloys are higher than 1500 K; with regard to the ratio T/Tf lower than 0.2, it is assumed that strain rates have little effects and the materials behaviours are considered as insensitive to strain rates in a first approach.
Finally, lubricants affect the drawing but lubrication is supposed homogeneous and constant during the process. Thus variations in lubrication are not taken into account and only a friction coefficient will be used to model friction.
Then, an elastoplastic constitutive equation is applied to model the materials behaviour, thus it is important to characterize this plastic behaviour. In this way, simple tests are performed.

Physical modelling

Materials Behaviour

The two studied materials (a stainless steel (316LVM) and a cobalt alloy (L605)) have a large ductility and can be cold formed.

TABLE 3. Elastic properties of the tube and tools materials.

Materials	Young Modulus GPa	Poisson Coefficient
316LVM	210	0.3
L605	210	0.3
PCD	950	0.2
WC	650	0.2

Only tensile tests are available for thin-wall tubes. They are easy to realize, but they are not sufficient to understand the material behaviour during drawing. Indeed tensile tests permit to observe only one strain direction and are not sufficient to correctly define the hardening law. Thus, cycling tensile tests have been realized for each material and the stress-strain curves are reported in the figures 4 and 5. They have been performed to observe the elastic springback during unloading: tension up to 700 MPa, reducing stress down to zero followed by a tension until breaking point.
An almost perfectly linear elastic springback is obtained during unloading and the reloading curve is very close to the unloading one. These tests lead up to apply in a first approach an elastoplastic constitutive equation with an isotropic hardening law. The elastic behaviour is described by Young's modulus and Poisson's ratio. The true strain-true stress curve describes the plastic behaviour.

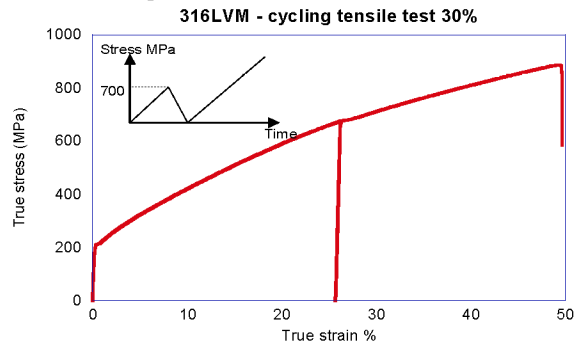

FIGURE 4. Stress-strain curve of the 316LVM cycling test.

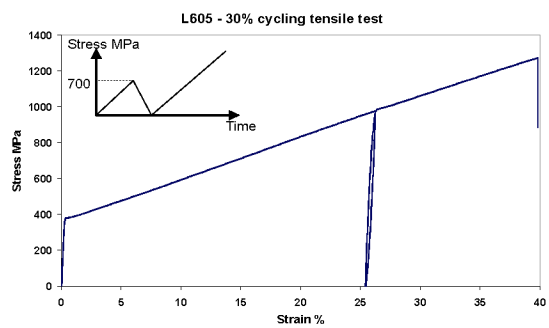

FIGURE 5. Stress-strain curve of the L605 cycling test.

Tools Behaviour

Dies are in diamond (PCD) and plugs are in tungsten carbide (WC). They were assumed to deform elastically because of their high elastic limit. Moreover no plastic deformation has ever been observed on tools after a drawing. Their elastic properties are listed in table 3.

Friction

The friction coefficient depends on a lot of parameters (materials, lubricants, surfaces…) and it is

difficult to determine it. In metal forming, the Coulomb model accounts for the effects of friction. A shear stress limit could have been applied if there are large normal stresses. This model does not take into account the fluctuation of lubrication. The Coulomb coefficient will be fit with the first simulation as it can be seen in the next paragraph.

Numerical Modelling

Load

Boundary conditions are shown in figure 6. They are the same as in experiments. Dies and plugs are fixed. Tube is drawn with a constant speed. In fact the speed has no influence here, as the model is quasi-static (cf. paragraph *Hypotheses*).

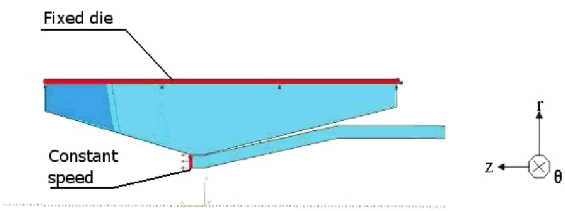

FIGURE 6. Boundary conditions of the drawing process model.

Meshing

Triangular elements are very versatile and convenient to mesh complex shapes. However, quadrilateral elements are able to provide an accurate solution at less cost. Quadrilateral elements have a better convergence than triangles but are less accurate if they are initially distorted (Abaqus 2006). In our case they are appropriate to mesh all instances except the dies. The use of quadratic elements does not modify results.
Consequently, tubes and plugs are meshed with 4-node axisymmetric continuum elements (CAX4). In order to fit well with geometry, dies are meshed mainly with the same elements but also with some triangular elements (CAX3). Quadratic elements were tested but their use does not improve the accuracy of the results.

Friction

A drawing process has been simulated with different friction coefficients and the numerical drawing forces are noted. It shows a linear dependence of the drawing force on the friction coefficient. Then, the 316LVM hollow sinkings have been used in order to define the friction coefficient. For each drawing, two simulations – one with a friction coefficient equal to zero and one equal to 0.25 – are realized to determine the Coulomb coefficient-drawing force curve (Figure 7). Then, the most appropriate coefficient, for which the numerical force is equal to the experimental force, is determined to be equal to 0.17. This coefficient value will be used for all the following simulations.
Besides, since the observed normal stresses are not too large, no shear stress limit is applied.

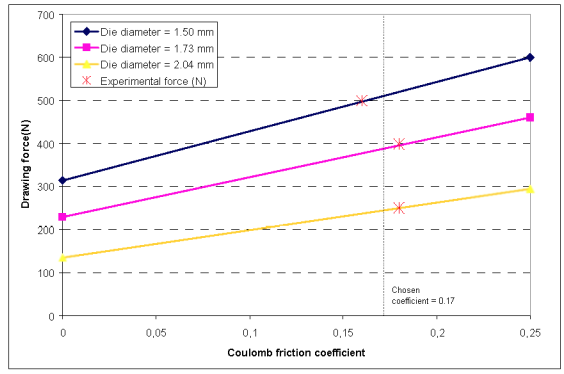

FIGURE 7. Influence of the Coulomb coefficient on the drawing force for a hollow sinking.

Convergence

These calculations involve nonlinearities due to large deformations and contacts, which make convergence complex. It can be necessary that an automatic stabilization for static problems should be employed to ease convergence for calculations. Here it is used only for fixed plug drawing calculations. The stabilization parameter, i.e. the damping factor, is problem-dependent and must be fitted so that the viscous energy dissipated by stabilization keeps negligible in comparison with the strain energy in the model. Then, checks of the results and the trimming of the damping factor are needed to trust these simulations.

COMPARISON DRAWING EXPERIMENTS-SIMULATION

Observations

Qualitatively, the same behaviours as in experimental process are noticed. First, in sinking, the tube peels off from the die, the centripetal flow continues a bit. The detachment is viewed in figure 8. It implies that sunken tube diameters are slightly lower than die diameters. The detachment is of the order of some hundredths of a millimetre (table 1).

Figure 9 presents the time evolution of the drawing force during a hollow sinking simulation. The three parts of the drawing are observed: an increase of the drawing force, a steady state and a decrease. In Figure 9, the simulated tube length is only 10 mm so the steady state is short. The drawing force is noted during the steady state.

Moreover, two compression points on the die can also be seen in figure 9. They take place where the tube changes direction and creates stress in the die. Damages are also observed here on real dies on which wear rings are generated during drawing process (Figure 10).

Finally, in hollow sinking, the tube is not constrained inside, so the thickness increases to make the reduction of diameters easier.

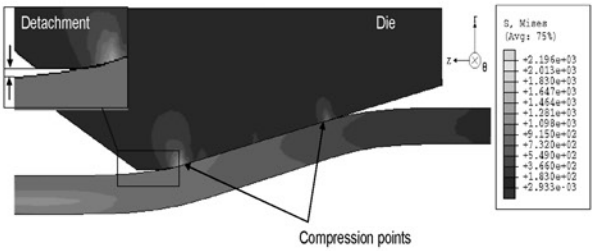

FIGURE 8. Observations of a finite element simulation of a hollow sinking tube process.

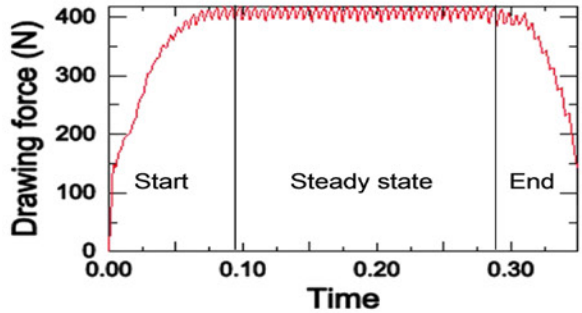

FIGURE 9. Evolution of the drawing force according to time for a hollow sinking test.

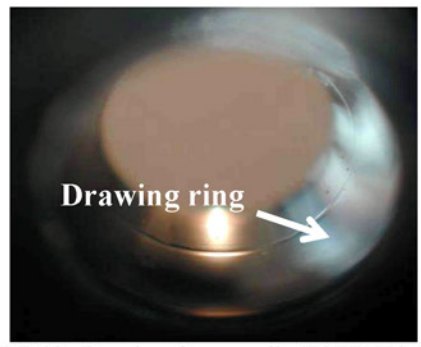

FIGURE 10. Drawing ring on a die (ESTEVES-DWD).

Hardening law

Isotropic hardening has been chosen to describe the material behaviour but the tensile tests are not sufficient to be sure of the hardening law. That's why other hardening models are tested to observe the difference between the results.

Three hardening models are applied: isotropic, linear kinematic and non linear kinematic hardening. In each case, three die diameters are tested and tube dimensions (Φext×Φint) are noted and compared with experimental measurements in the table 4. It can be noted that the hardening model has a great influence on the final geometries. For kinematic hardening, linear or not, the elastic springback is very important

TABLE 4. Influence of hardening model on the final tube geometry after a hollow sinking test.

Die diameters (mm)		1.50	1.73	2.04
Experimental measurements		1.47×1.07	1.70×1.30	1.98×1.58
Hardening type	Isotropic	1.41×1.02	1.65×1.26	1.96×1.58
	Linear kinematic	1.73×1.38	1.94×1.59	2.02×1.65
	Non linear kinematic	/	1.76×1.39	2.07×1.69

TABLE 5. Comparison between the results predicted by the FE model and the experience measurements for L605 hollow sinking.

Die Angle	Die Diameter (mm)	Outer Diameter (mm)			Inner diameter (mm)			Drawing Force (daN)		
		Model	Experiment	Error	Model	Experiment	Error	Model	Experiment	Error
25°	1.45	1.400	1.455	3.8%	1.127	1.181	4.6%	36	37	1.4%
25°	1.50	1.452	1.488	2.4%	1.180	1.208	2.3%	33	32	3.1%
25°	1.60	1.550	1.586	2.3%	1.280	1.312	2.4%	28	26	7.7%
14°	1.58	1.556	1.586	1.9%	1.288	1.322	2.6%	31	29	6.9%

TABLE 6. Comparison between the results predicted by the FE model and the experience measurements for drawing with fixed plug

Material	Drawing Force (daN)			Plug force (daN)		
	Model	Experiment	Error	Model	Experiment	Error
316LVM	700	625	12%	120	120	0%
L605	580	470	23%	105	100	5%

and the final tubes dimensions are far from the experimental ones. It appears that the isotropic hardening leads to the results which are the closest from experimental values. So it seems to confirm the choice of an isotropic hardening.

Comparative Statement

Hollow Sinking

L605 tube drawing has been modelled with the same parameters as 316LVM. An isotropic hardening and a 0.17 friction coefficient has been applied. Like in experiments, inner and outer initial diameters are respectively 1.81×2.06 mm.

All the results are listed in table 5. For each drawing, die geometry is noted. The outer and inner diameters as well as the drawing forces are obtained in the simulation. Then the data predicted by the FE model and the experimental measurements are confronted and the error is noted in percentage. The estimated geometries show good correlation with the experimental measurements. The average error on the geometries for L605 hollow sinking is about 2.8%. With an average error of 4.8%, the drawing force obtained is also in good agreement with reality, which indicates that the chosen Coulomb coefficient is also pertinent for the contact L605-PCD.

Drawing With Fixed Plug

Two drawings with fixed plug have been modelled, one with 316LVM and one with L605. The friction coefficient is taken again equal to 0.17.

Stabilization is used for these calculations. Several calculations have been realized to fit the damping factor. The most appropriate values for this factor are equal to 0.05 and 0.1 for 316LVM and L605, respectively. These values permit calculations to converge while viscous forces stay negligible in comparison with the other forces.

Dimensions and forces have been compared with experiments. The numerical and the experimental forces as well as the error between them are listed in the table 6. On the one hand, drawn tube diameters are equal to tools diameters in modelling and in experiments so the dimensional accuracy is good. The detachment phenomenon is not present because of the plug. The forces applied on the die are also correct. On the other hand drawing force is overestimated in the model. The overestimation of the drawing force is nearly 17%. This may be due to the numerical stabilization used in these calculations or to the friction coefficient with tungsten carbide.

CONCLUSIONS

Until now, only dimensions and forces data are observed and the results are encouraging. An elastoplastic constitutive equation with an isotropic hardening is applied with a Coulomb friction coefficient of 0.17. Hollow sinking FE model is in good agreement with experimental measurements. Dimensions predicted by the FE model are also good for fixed plug drawing as well, but the predicted forces are overestimated. It may be due to the determination of the materials plasticity model. The stress-strain curves obtained by tensile tests are limited and do not account entirely for the materials behaviour. Indeed during the drawing, the material undergoes two strains: a longitudinal tension and a radial compression. In drawing with plug, the radial compression is large, that's why the forces predicted by the FE model are less accurate than in hollow sinking. Then, a better experimental test must be used. An adapted test would be a tensile test with radial compression at the same time but its realization is difficult. An equivalent of these two strains is the shearing. It seems to be easier to realize and is at the planning stage to define better the material behaviour.

Besides, for the contacts with tungsten carbide, the same coefficient (0.17) has been chosen as for PCD. However, several coefficients for the contact tube-plug have been tested and their influence on the drawing force has not been significant.

Finally numerical stabilization is also a source of mistakes. It induces overestimated results. Indeed, it causes an increase of the stresses and consequently of the forces. Even if the energy dissipated by the stabilization is checked to be insignificant, drawing forces predicted by the FE model with plug are too large and far from the average error of hollow sinking model. Thus the overestimation due to stabilization must be quantified to ensure it can be used.

REFERENCES

1. Um, K., and Lec, D. N., *J. Mater. Process. Technol.* **63,** 43-48 (1997).
2. Neves, F. O., Button, S. T., Caminaga, C., and Gentile, F. C., *J. of the Braz. Soc. Of Mech. Sci. & Eng.*, **XXVII, A**, 426-431 (2005).
3. Yoshida, K., and Furuya, H., *J. Mater. Process. Technol.* **153-154**, 145-150 (2004).
4. Yoshida, K., Watanabe, M., and Ishikawa, H., *J. Mater. Process. Technol.* **118**, 251-255 (2001).
5. Karnezis, P., and Farrugia, D. C. J., *J. Mater. Process. Technol.* **80-81**, 690-694 (1998).
6. Abaqus v. 6.6 "21.1.1 Solid (continuum) elements" in *Abaqus Analysis user's manual,* 2006.